NOVEL ALGORITHM FOR EARTH-FAULT LOCATION IN COMPENSATED MV-NETWORKS

Janne ALTONEN, Ari WAHLROOS
ABB Oy Medium Voltage Products – Finland
janne.altonen@fi.abb.com, ari.wahlroos@fi.abb.com

ABSTRACT

This paper presents a novel earth-fault location algorithm, which enables the estimation of the earth-fault distance in compensated MV-networks. The novelty of the algorithm is that the fault location can be calculated with reduced number of settings compared to prior-art methods. This improves the practical usability and accuracy of the earth-fault location.

The key idea of the novel algorithm is to provide a set of equations based on an equivalent circuit valid for single-phase earth fault so that for the first time four unknown variables can be determined, that is, the fault distance and fault resistance, but also the conductance and susceptance parts of the shunt admittance of the protected line. Until now it has been mandatory to give the shunt admittance value of the protected line as a setting to enable impedance based fault location computation in compensated MV-networks. With the suggested algorithm the earth-fault distance can be estimated without setting the shunt admittance value, although its influence is included in the method.

In the paper, the basic theory of modeling the phase-to-earth fault loop and the challenges related to it are shortly reviewed first. Secondly, the theory of the novel algorithm is introduced. Finally, the performance of the novel algorithm is compared to one of the prior-art solutions. This is done using data from comprehensive field tests conducted in a typical rural 20 kV overhead line network with central compensation. The results clearly demonstrate the significance of the shunt admittance parameter in providing meaningful results when the prior-art methods are used. The results also show that the novel algorithm extends the application of computational fault location in terms of fault resistance from solid earth faults into low-impedance earth faults. However, the practically achievable maximum fault resistance of an earth fault that can be located with adequate accuracy is limited e.g. by the practical measurement accuracy of the whole measurement chain including the measurement transformers and the IED.

INTRODUCTION

The computational location of earth faults in compensated MV-networks has been the subject of research and development in recent years in order to find a practical solution to be implemented within modern IEDs and DMS.

It is common for the prior-art techniques using fundamental frequency phasors to utilize changes in measured voltages and currents during the fault in the fault distance calculation. In practice, these changes can be accomplished e.g. by switching on or off the parallel resistor of the compensation coil during the fault. The fault distance and fault resistance can then be determined using equations based on an appropriate equivalent circuit [1, 2 and 3]. Further, it is common for the prior-art methods that the shunt admittance of the protected line must be given as a setting value. One of the major practical challenges is that this value is not constant in practice. It changes whenever the configuration of the protected line changes and in overhead line networks it is even somewhat dependable on weather conditions.

Another practical challenge of earth-fault location in compensated MV-networks is the fault resistance magnitude which may vary considerably. This is demonstrated in *Fig. 1*, which shows results from a study regarding the fault resistance distribution of earth faults occurred in a compensated and unearthed MV-distribution network over a one year period [4]. According to this study solid and low-ohmic earth faults (R_F < 500 Ω) present a considerable share of the total number of faults in practice.

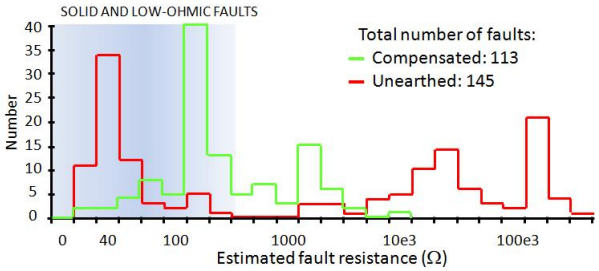

Fig. 1 *Fault resistance distribution of earth faults in a compensated and unearthed MV-network [4].*

The fault location estimation of purely solid earth faults is not sensitive to the correctness of the set shunt admittance value. But as the fault resistance increases from solid to low-ohmic level this sensitivity becomes very high. One example of this kind of behaviour is shown in reference [1] where the performance of one of the prior-art methods has been analysed. It can be concluded that the required setting accuracy to enable satisfactory location of low-ohmic faults exceeds the practically available accuracy, e.g. based on data available in DMS or approximations provided in technical publications.

In order to eliminate this problematic setting parameter an improved algorithm is introduced. The motivation is also to extend the application of earth-fault location so that a bigger share of the total number of permanent solid and low-ohmic earth faults could be located. With the suggested algorithm the earth-fault distance can be estimated without setting the shunt admittance value, although its influence is included in the method. However, it should be emphasized that in practice when the measured impedance loop becomes dominantly resistive due to fault resistance ($R_{LOOP}+R_F >> X_{LOOP}$), the sensitivity of any fundamental frequency impedance based

algorithm to the correct setting parameters and measurement signals becomes exceptionally high. Even a small measurement error, e.g. in the phase angle of the estimated fault loop impedance, results in a large error in the fault loop reactance, i.e. in the distance estimate. To mitigate these errors special attention must be paid on the accuracy of both the measurements and the settings.

PHASE-TO-EARTH FAULT LOOP MODELING

Fundamental frequency impedance based fault distance calculation is based on estimating the reactance of the so called phase-to-earth fault loop. When calculating the impedance of this fault loop the voltage across it and the current flowing through it must be estimated with adequate accuracy. One example of fault loop modeling during an earth fault in no-load conditions is shown in *Fig. 2*.

The following notations are used in *Fig. 2*:

d = Per unit fault distance (d = 0…1 p.u.).
$\underline{Z}_1$ = Positive-sequence impedance of the protected feeder.
$\underline{Z}_2$ = Negative-sequence impedance of the protected feeder.
$\underline{Z}_0$ = Zero-sequence impedance of the protected feeder.
$\underline{Y}_0$ = Phase-to-earth admittance of the protected feeder per phase.
$\underline{Y}_{0Bg}$ = Phase-to-earth admittance of the background network per phase.
R_F = Fault resistance at the fault point.
$\underline{I}_1$ = Positive-sequence current measured at IED location.
$\underline{I}_2$ = Negative-sequence current measured at IED location.
$\underline{I}_0$ = Zero-sequence current measured at IED location.
$\underline{I}_{0Fd}$ = Zero-sequence charging current of the feeder.
q = Distribution factor for zero-sequence current of the feeder.
$\underline{I}_F$ = Fault component current at the fault point (actual fault current is $3\cdot\underline{I}_F$).
$\underline{U}_1$ = Positive-sequence voltage measured at IED location.
$\underline{U}_2$ = Negative-sequence voltage measured at IED location.
$\underline{U}_0$ = Zero-sequence voltage measured at IED location.
$\underline{U}_{ph} = \underline{U}_0 + \underline{U}_1 + \underline{U}_2$ = Phase-to-earth voltage measured at IED location.

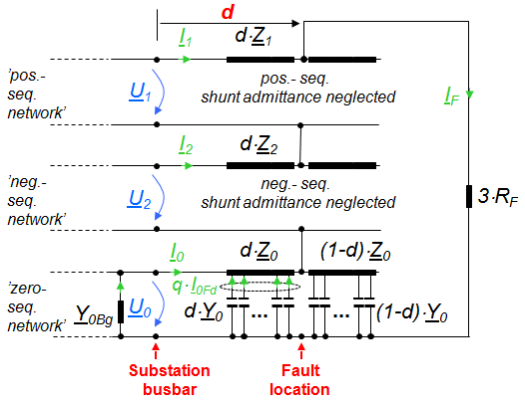

Fig.2 *Simplified equivalent circuit model for phase-to-earth fault loop during no-load conditions using sequence components.*

Based on the equivalent circuit of *Fig. 2* the following equations can be written:

$$\underline{U}_{ph} = \underline{U}_0 + \underline{U}_1 + \underline{U}_2 = d\cdot\underline{Z}_0\cdot(\underline{I}_0 + q\cdot\underline{I}_{0Fd}) + d\cdot\underline{Z}_1\cdot\underline{I}_1 + \ldots \quad (1)$$
$$d\cdot\underline{Z}_2\cdot\underline{I}_2 + 3\cdot R_F\cdot\underline{I}_F$$

$$\underline{I}_F = \underline{I}_0 + \underline{I}_{0Fd} = \underline{I}_0 - \underline{U}_0\cdot\underline{Y}_0 \quad (2)$$

In this model the measured positive- and negative-sequence currents simply flow through the corresponding line impedances from the substation to the fault point, but for the zero-sequence the modeling becomes more complex. The current flowing through the zero-sequence impedance $d^*\underline{Z}_0$ is composed of two parts. The first part is due to the zero-sequence current $\underline{I}_0$ fed by the background network. The second part is due to the zero-sequence current produced by the protected line $\underline{I}_{0Fd}$, which must be estimated as it cannot be measured directly. This estimation is based on the fact that the contribution of the zero-sequence current $\underline{I}_{0Fd}$ on the voltage drop over the corresponding impedance $d^*\underline{Z}_0$ depends on the fault location and on the shunt admittance $\underline{Y}_0$ and its distribution along the protected line, *Fig.2*. Parameter q is used as a distribution factor for the current $\underline{I}_{0Fd}$. In practice, the parameter q represents how the shunt admittance is distributed along the line, e.g. evenly distributed shunt admittance means that q equals 0.5. Finally, the fault component current $\underline{I}_F$, which represents the actual fault current in the fault spot, can be estimated as a sum of the currents $\underline{I}_0$ and $\underline{I}_{0Fd}$.

For the voltage drop calculation the shunt admittance $\underline{Y}_0$ of the protected line needs to be known and a value for the q parameter must be given. Principally, by dividing *Eq.1* into real and imaginary parts the fault distance d and fault resistance R_F can be easily solved. As in practice the sequence components are also affected by the load current and asymmetry of the network, it is advisable to use so called delta quantities in the calculations in order to improve the fault location accuracy [1]. This means that the current and voltage phasors in *Eq. 1* and *2* are replaced by the corresponding changes during the fault or due to the fault.

NOVEL ALGORITHM THEORY

The novel algorithm is based on the idea of providing not two, but four equations based on an equivalent circuit valid for single-phase earth fault. This can be accomplished by utilizing the time instants before and after the change during the fault, and by dividing the resulting equations into real and imaginary parts.

Using the equivalent circuit of *Fig. 2*, *Eq. 1* and *2* can be re-written in the following way:

$$\underline{U}_{ph\_t1} = d\cdot\underline{Z}_0\cdot(\underline{I}_{0\_t1} + I_{0Fd\_t1}\cdot q) + d\cdot\underline{Z}_1\cdot\underline{I}_{1\_t1} + \ldots \quad (3)$$
$$d\cdot\underline{Z}_2\cdot\underline{I}_{2\_t1} + 3\cdot R_F\cdot I_{F\_t1}$$

$$\underline{U}_{ph\_t2} = d\cdot\underline{Z}_0\cdot(\underline{I}_{0\_t2} + I_{0Fd\_t2}\cdot q) + d\cdot\underline{Z}_1\cdot\underline{I}_{1\_t2} + \ldots \quad (4)$$
$$d\cdot\underline{Z}_2\cdot\underline{I}_{2\_t2} + 3\cdot R_F\cdot I_{F\_t2}$$

$$\underline{I}_{F\_t1} = \underline{I}_{0\_t1} + \underline{I}_{0Fd\_t1} = \underline{I}_{0\_t1} - \underline{U}_{0\_t1}\cdot\underline{Y}_0 \quad (5)$$

$$\underline{I}_{F\_t2} = \underline{I}_{0\_t2} + \underline{I}_{0Fd\_t2} = \underline{I}_{0\_t2} - \underline{U}_{0\_t2}\cdot\underline{Y}_0 \quad (6)$$

The subscripts t_1 and t_2 relate to time instants during the fault before and after the change. Other notations are as used in *Fig. 2*.

As in reality the measured sequence components in *Eqs. 3-4* are affected by load, the concept of equivalent load tap and its distance can be applied in the modeling [5]. This means that the whole load of the line can be modeled into a single load tap located at equivalent load distance s [p.u.] from the substation. Therefore, *Eqs. 3-4* are only valid in case the fault is located in front of the equivalent load tap ($d < s$). If the fault is located behind the equivalent load tap ($d \geq s$), *Eqs. 7-8* are valid instead.

$$\underline{U}_{ph\_t1} = d \cdot \underline{Z}_0 \cdot (\underline{I}_{0\_t1} + \underline{I}_{0Fd\_t1} \cdot q) + s \cdot \underline{Z}_1 \cdot \underline{I}_{1\_t1} + \ldots \quad (7)$$
$$(d-s) \cdot \underline{Z}_1 \cdot \underline{I}_{F\_t1} + s \cdot \underline{Z}_2 \cdot \underline{I}_{2\_t1} + (d-s) \cdot \underline{Z}_2 \cdot \underline{I}_{F\_t1} + 3 \cdot R_F \cdot \underline{I}_{F\_t1}$$

$$\underline{U}_{ph\_t2} = d \cdot \underline{Z}_0 \cdot (\underline{I}_{0\_t2} + \underline{I}_{0Fd\_t2} \cdot q) + s \cdot \underline{Z}_1 \cdot \underline{I}_{1\_t2} + \ldots \quad (8)$$
$$(d-s) \cdot \underline{Z}_1 \cdot \underline{I}_{F\_t2} + s \cdot \underline{Z}_2 \cdot \underline{I}_{2\_t2} + (d-s) \cdot \underline{Z}_2 \cdot \underline{I}_{F\_t2} + 3 \cdot R_F \cdot \underline{I}_{F\_t2}$$

The shunt admittance $\underline{Y}_0$ can be written in the following form:

$$\underline{Y}_0 = k \cdot B_0 + j \cdot B_0 \quad (9)$$

$$k = \frac{real(\overline{Y}_0)}{imag(\overline{Y}_0)},$$

where k is the ratio of real and imaginary parts of $\underline{Y}_0$.

The voltage and current terms in *Eq. 3, 5* and *7* are preferably selected as $\underline{U}_{ph\_t1} = \underline{U}_{ph\_t1}$, $\underline{U}_{0\_t1} = \Delta\underline{U}_{0\_t1}$, $\underline{I}_{1\_t1} = \underline{I}_{1\_t1}$, $\underline{I}_{2\_t1} = \Delta\underline{I}_{2\_t1}$, $\underline{I}_{0\_t1} = \Delta\underline{I}_{0\_t1}$, $\underline{I}_{F\_t1} = \Delta\underline{I}_{F\_t1} = \Delta\underline{I}_{0\_t1} + \Delta\underline{I}_{0Fd\_t1}$, $\underline{I}_{0Fd\_t1} = \Delta\underline{I}_{0Fd\_t1}$ and in *Eq. 4, 6* and *8* as $\underline{U}_{ph\_t2} = \underline{U}_{ph\_t2}$, $\underline{U}_{0\_t2} = \Delta\underline{U}_{0\_t2}$, $\underline{I}_{1\_t2} = \underline{I}_{1\_t2}$, $\underline{I}_{2\_t2} = \Delta\underline{I}_{2\_t2}$, $\underline{I}_{0\_t2} = \Delta\underline{I}_{0\_t2}$, $\underline{I}_{F\_t2} = \Delta\underline{I}_{F\_t2} = \Delta\underline{I}_{0\_t2} + \Delta\underline{I}_{0Fd\_t2}$, $\underline{I}_{0Fd\_t2} = \Delta\underline{I}_{0Fd\_t2}$, where Δ indicates a change from pre-fault to fault conditions.

Finally, based on the above four equations totally four unknown variables can be solved: d, R_F, B_0 and k. The logic for selecting between the results from *Eqs. 3-4* and *7-8* is based on the calculated fault distance estimates: if d of *Eqs. 3-4* is less than s, this is the valid fault distance estimate; otherwise the distance estimate is taken from *Eqs. 7-8*. This modeling method has the advantage that it enables the fault distance estimation without setting the shunt admittance value, and the inaccuracy caused by the deviation in it can now be eliminated from the results. This approach also eliminates the requirement to approximate how the shunt admittance is distributed along the line (setting parameter q), which can be considered as another major benefit. From the end-user point of view, there is therefore no longer need to determine, set and update the shunt admittance parameter if the switching state of the protected line changes.

FIELD TESTING AND EXPERIENCE

Test arrangement

In order to compare the performance of the novel earth-fault location algorithm with the prior-art method presented in reference [1], one trial earth-fault test series is studied. The tests were performed in a compensated 20 kV network owned by Savon Voima Verkko Oy, Finland. During the tests three feeder configurations (*a*, *b* and *c*) and the three fault locations as shown in *Fig. 3* were used. Tests at the fault location #1 and #3 were done with the configuration *a*, whereas at the fault location #2 configurations *b* and *c* were used. Both solid and low-ohmic earth faults using a 500 Ω artificial fault resistor were conducted in all fault locations. The change during the earth fault was accomplished by connecting a 4 A (at 20 kV) resistor in parallel with the compensation coil after a time delay.

The line impedances of the test feeder were measured from the substation to the fault locations #2 and #3 in order to validate the initial line data stored in DMS [1]. For the fault location #1 the impedances were obtained based on DMS data. *Table 1* shows the actual line impedances from the substation to all fault locations.

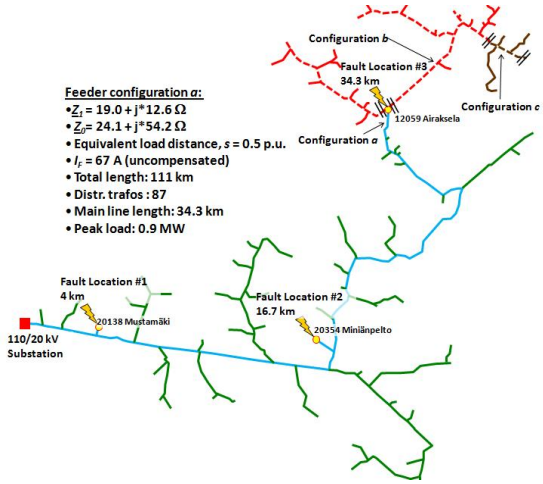

Fig. 3 *Test feeder configuration. The main line is marked with blue colour, and the extensions in line length are marked with red and brown colour.*

Table 1. *Actual line impedances from the substation to the fault locations based on primary measurements (#2 and #3) and on DMS data (#1).*

Fault location	d (km)	d (p.u.)	$\underline{Z}_1$ (Ω)	$\underline{Z}_0$ (Ω)
#3	34.3	1.00	19.0+j·12.6	24.1+j·54.2
#2	16.7	0.52	9.1+j·6.2	11.5+j·29.4
#1	4.0	0.12	1.5+j·1.5	2.1+j·7.0

For the current measurements conventional CTs were used, but voltages were measured with resistive voltage dividers, i.e. with sensors [1]. In order to minimize measurement related errors in the analysis error-compensated signals from oscilloscope were used in the calculations.

The total shunt admittance of the test feeder was measured by conducting earth-fault tests outside of it [1]. This was done only during the feeder configuration *a*. For the other feeder configurations the measured shunt admittance value was scaled according to the total line lengths available in DMS data. *Table 2* shows the estimated values valid for the different feeder configurations, which are required as a setting parameter for the evaluated prior-art method. However, for the novel method this setting is not required.

Table 2. *Results of the shunt admittance estimation of the test feeder.*

Feeder configuration	abs(3*$\underline{I}_{0Fd}$) (A) at 20kV	re($\underline{Y}_0$) (mS)	im($\underline{Y}_0$) (mS)
a	6.81	0.00235	0.197
b	8.88	0.00307	0.256
c	9.42	0.00325	0.272

Performance evaluation and comparison

The fault distance and fault resistance estimates utilizing the prior-art method [1] and the novel method were calculated for all fault locations (F.L.). For the impedance setting the value valid for the main line (feeder configuration *a*) was used, *Table 1*. This setting is required for both methods, and the given value was used despite the changes in the feeder configuration. The shunt admittance values required as setting for the prior-art method are shown in *Table 2*.

A solid and low-ohmic earth fault at the fault location #3 is presented in detail in *Fig. 4a* and *4b*. Both the waveforms of the residual quantities and the resulting fault distance and fault resistance estimates calculated with both methods are shown. The shaded areas represent the time window where mean values for the current and voltage quantities at time instants t_1, t_2 and t_{pre} are calculated. For the prior-art method the fault

distance calculation was repeated with three setting values of $\underline{Y_0}$, which equal 1.0, 1.05 and 0.95 times the correct value valid for the feeder configuration in question. It can be seen that the distance estimates given by the prior-art method are greatly affected by the $\underline{Y_0}$ setting, as the fault resistance increases. Whereas the distance estimates given by the novel method are independent of the $\underline{Y_0}$ value of the line. Also both methods provide fairly accurate fault resistance estimates, which can be utilized in the validity judgement and error compensation of the fault distance estimate [1].

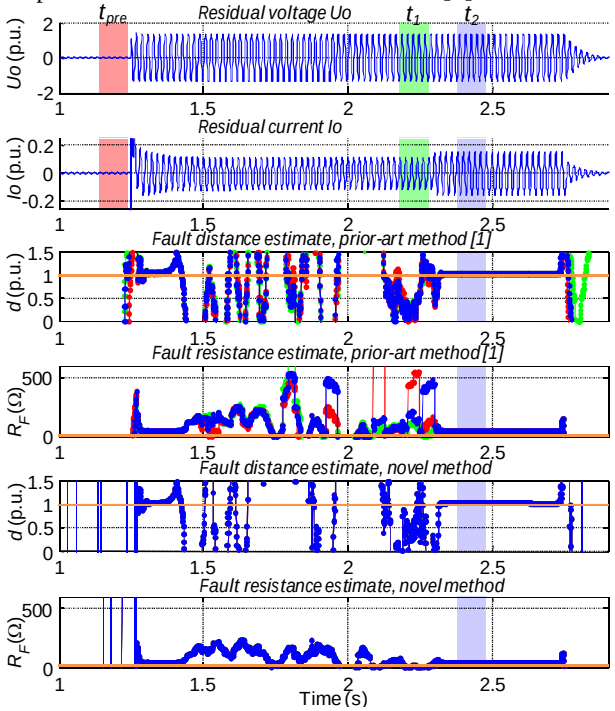

Fig. 4a *Performance of the methods in a solid earth fault at F.L. #3.*

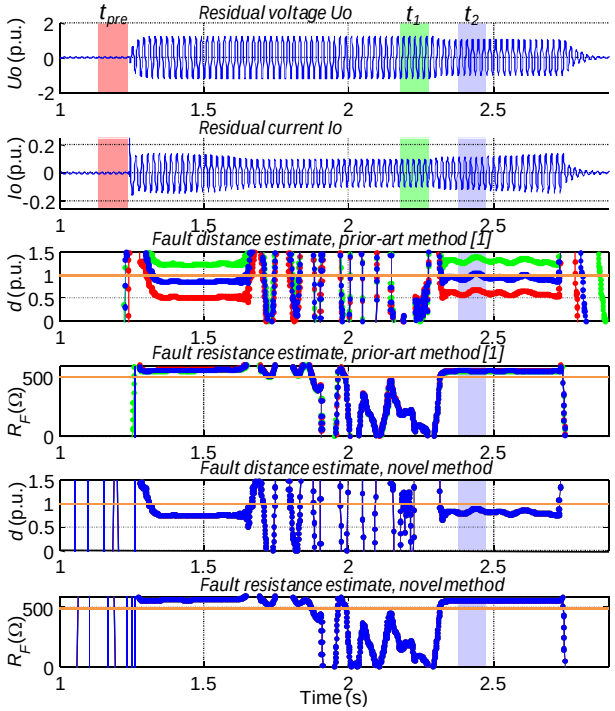

Fig. 4b *Performance of the methods in a 500 Ω -earth fault at F.L. #3.*

The results obtained above from the fault location #3 together with those from the fault locations #1 and #2 are summarized in *Table 3a*, *3b* and *3c*. From *Table 3a* and *3c* it can be seen that in case of solid earth faults both methods provide good results and a ±5% deviation in the $\underline{Y_0}$ setting of the prior-art method does not affect the accuracy. But in case of 500 Ω-faults the ±5% deviation in the $\underline{Y_0}$ setting makes the results from the prior-art method unusable, but the novel method still provides meaningful results. The errors clearly increase with the fault resistance, but as the magnitude and direction of the error is almost the same in each fault location, *Table 3c*, it could be easily compensated and taken account for.

The analysis also revealed that the fault location estimation is also affected by the faulted phase due to the natural asymmetry of the network parameters. To fully eliminate the influence of this asymmetry more enhanced fault loop model would be required.

Table 3a. *Fault distance estimates for solid earth faults calculated with the prior-art method [1], which requires the $\underline{Y_0}$ setting*

F.L.	***d* (p.u.) [1] R_F = 0 Ω**			***error* (p.u.)**		
	$\underline{Y_0}$ setting (p.u.)			$\underline{Y_0}$ setting (p.u.)		
	1.00	*1.05*	*0.95*	*1.00*	*1.05*	*0.95*
#1	0.17	0.17	0.17	0.05	0.05	0.05
#2	0.52	0.52	0.52	0.00	0.00	0.00
#3	1.02	1.02	1.01	0.02	0.02	0.01

Table 3b. *Fault distance estimates for low-ohmic faults calculated with the prior-art method [1], which requires the $\underline{Y_0}$ setting*

F.L.	***d* (p.u.) [1] R_F = 500 Ω**			***error* (p.u.)**		
	$\underline{Y_0}$ setting (p.u.)			$\underline{Y_0}$ setting (p.u.)		
	1.00	*1.05*	*0.95*	*1.00*	*1.05*	*0.95*
#1	0.06	~~0.34~~	~~-0.21~~	-0.06	~~0.22~~	~~-0.33~~
#2	0.41	~~0.80~~	~~0.04~~	-0.11	~~0.28~~	~~-0.48~~
#3	0.96	~~1.31~~	~~0.61~~	-0.04	~~0.31~~	~~-0.39~~

Table 3c*. Fault distance estimates for solid and low-ohmic faults calculated with the novel method, which does not require the $\underline{Y_0}$ setting.*

F.L.	***d* (p.u.) [1] R_F = 0 Ω**	***error* (p.u.) R_F = 0 Ω**	***d* (p.u.) [1] R_F = 500 Ω**	***error* (p.u.) R_F = 500 Ω**
#1	0.17	0.05	-0.04	-0.16
#2	0.51	-0.01	0.36	-0.16
#3	1.01	0.01	0.82	-0.18

[1] Per unit fault distance is based on the loop reactance setting selected according to fault location #3 ($X_{LOOP} = (2 \cdot X_1 + X_0)/3 = 26.5\ \Omega$)

CONCLUSIONS

The algorithm introduced in this paper is a true step forward in finding a practical solution for the computational location of earth faults in compensated medium voltage networks. Since, to date, IEDs available in the global power distribution market have totally been lacking in solutions for this application, ABB will in the near future be implementing this functionality within the product portfolio for medium voltage applications. This decision is also further justified by the very promising performance results obtained from field tests.

REFERENCES

[1] Altonen J., Wahlroos A.,"*Advancements in earth-fault location in compensated networks*", CIRED 2011, Frankfurt

[2] Hänninen S., Lehtonen M.,"*Earth fault distance computation with fundamental frequency signals based on measurements in substation supply bay*", VTT Research Notes 2153, Espoo 2002

[3] Schegner P., Eberl G.,"*Computation of the earth fault distance in compensated MV-networks by evaluating steady state values*", PSCC 2002, Sevilla

[4] Hänninen S.,"*Single phase earth faults in high impedance grounded system. Characteristics, indication and location*", VTT Energy, 2001

[5] Altonen J., Wahlroos A.,"*Advancements in fundamental frequency impedance based earth-fault location in unearthed distribution networks*", CIRED 2007, Vienna